# DNA instability in postmitotic neurons

**Roman Gonitel*, Hilary Moffitt*, Kirupa Sathasivam*, Ben Woodman*, Peter J. Detloff†, Richard L. M. Faull‡, and Gillian P. Bates*§**

*Department of Medical and Molecular Genetics, King's College London School of Medicine, London SE1 9RT, United Kingdom; †Department of Biochemistry and Molecular Genetics, University of Alabama at Birmingham, Birmingham, AL 35294; and ‡Department of Anatomy with Radiology, Faculty of Medicine and Health Science, University of Auckland, Private Bag 92019, Auckland, New Zealand

Communicated by David E. Housman, Massachusetts Institute of Technology, Cambridge, MA, January 3, 2008 (received for review December 10, 2007)

**Huntington's disease (HD) is caused by a CAG repeat expansion that is unstable upon germ-line transmission and exhibits mosaicism in somatic tissues. We show that region-specific CAG repeat mosaicism profiles are conserved between several mouse models of HD and therefore develop in a predetermined manner. Furthermore, we demonstrate that these synchronous, radical changes in CAG repeat size occur in terminally differentiated neurons. In HD this ongoing mutation of the repeat continuously generates genetically distinct neuronal populations in the adult brain of mouse models and HD patients. The neuronal population of the striatum is particularly distinguished by a high rate of CAG repeat allele instability and expression driving the repeat upwards and would be expected to enhance its toxicity. In both mice and humans, neurons are distinguished from nonneuronal cells by expression of MSH3, which provides a permissive environment for genetic instability independent of pathology. The neuronal mutations described here accumulate to generate genetically discrete populations of cells in the absence of selection. This is in contrast to the traditional view in which genetically discrete cellular populations are generated by the sequence of random variation, selection, and clonal proliferation. We are unaware of any previous demonstration that mutations can occur in terminally differentiated neurons and provide a proof of principle that, dependent on a specific set of conditions, functional DNA polymorphisms can be produced in adult neurons.**

CAG repeat instability | differentiated neuron | Huntington's disease | mismatch repair | somatic mutation

Tandem DNA repeats are mutational hotspots in the genome for which variability in length can produce physiological phenotypic differences that may contribute to rapid evolution of species-typical traits (1, 2) and on expansion are known to cause a large number of diseases (3). Instability of expanded repeats, a change in repeat number, occurs on intergenerational transmission and in somatic tissues and can be observed as mosaicism (heterogeneity of the repeat length in the tissue). Because repeat length variability can produce phenotypic diversity, somatic instability of tandem repeats can be a source of cellular diversity both physiologically and pathologically.

Huntington's disease (HD) is caused by a CAG repeat expansion for which mosaicism in the somatic tissues of HD mouse models (4–7) and in HD patient brains (8, 9) has been widely reported. Observations that the repeat continues to be unstable in adult mouse brains led to a hypothesis that somatic instability may contribute to the disease process and that the repeats could be unstable in nondividing neurons (5, 9). Previous studies have demonstrated divergence in the CAG repeat length between brain cell types. In dentato-rubral pallido-luysian atrophy post mortem brains, granule cells were found to have shorter repeats than Purkinje cells and both were shorter than those in glia (10, 11). In HD patients and a knockin HD mouse model, neuronal alleles, on average, were found to be longer than glial alleles (12). However, in all of these studies the median differences between the neuronal and nonneuronal cell populations were small, usually not exceeding more than five repeat units.

Therefore, CAG repeat mosaicism in neuronal populations in dentato-rubral pallido-luysian atrophy and HD postmortem brains has been shown, but, crucially, it has not been established when and where these diverse alleles are generated: in replicating neuronal progenitor cells or in nonreplicating terminally differentiated neurons. Similarly, there has been no indication of the causes that predispose cells to differential rates of CAG instability. In this study we set out to determine whether the instability leading to CAG repeat mosaicism has occurred in terminally differentiated neurons and to understand how differences in instability rates arise between cell populations.

## Results

**Signatures of Somatic CAG Instability in the Brain.** The R6/1 mouse model of HD expresses exon 1 of the human HD gene with ≈120 CAGs (13), and we have previously reported that the degree of somatic instability that occurs in this mouse model varies between brain regions and peripheral tissues (5). We sought to establish baseline CAG repeat size distribution profiles and their variability between individual mice (Fig. 1). Consistent with previous findings, mosaicism developed with age and was highly specific to brain region. Our multiple comparisons demonstrate that patterns of CAG repeat distribution are remarkably reproducible between individuals, implying that the mutation behaves in a predetermined manner. Each distribution contained two major components: one that changes little with time (conservative component) and a multimodal component that increases in size with age (radical component). The multimodality can be inferred from the appearance of numerous peaks within traces (Figs. 1–3). In the striatum and brainstem, the radical component is apparent at 3 months of age and expands with time at mode-specific rates. The tissue profiles differ by the relative proportion and position of the radical components and their modal composition (Figs. 1–3). We then conducted a similar detailed analysis of CAG repeat instability in brain regions of the R6/2 human exon 1 model (13) (≈210 CAGs) and the *Hdh*Q150 knockin model in which ≈150 CAGs have been knockin to the mouse HD gene (*Hdh*) (14, 15) [supporting information (SI) Fig. 6]. Comparison of repeat profiles among the three models reveals that the relative rate of CAG repeat instability and the modality of the CAG repeat size distribution for each brain region are conserved, generating a distinctive pattern or "signature" (Figs. 1 and 2).

We next examined CAG repeat distributions in the mRNA

Author contributions: R.G. and G.P.B. designed research; R.G., H.M., K.S., and B.W. performed research; R.G., K.S., B.W., P.J.D., and R.L.M.F. contributed new reagents/analytic tools; R.G., H.M., and G.P.B. analyzed data; R.G. and G.P.B. wrote the paper; and G.P.B. raised funds to support the research.

The authors declare no conflict of interest.

Freely available online through the PNAS open access option.

§To whom correspondence should be addressed at: Department of Medical and Molecular Genetics, King's College London School of Medicine, Eighth Floor, Guy's Tower, Guy's Hospital, London SE1 9RT, United Kingdom. E-mail: gillian.bates@genetics.kcl.ac.uk.

This article contains supporting information online at www.pnas.org/cgi/content/full/0800048105/DC1.

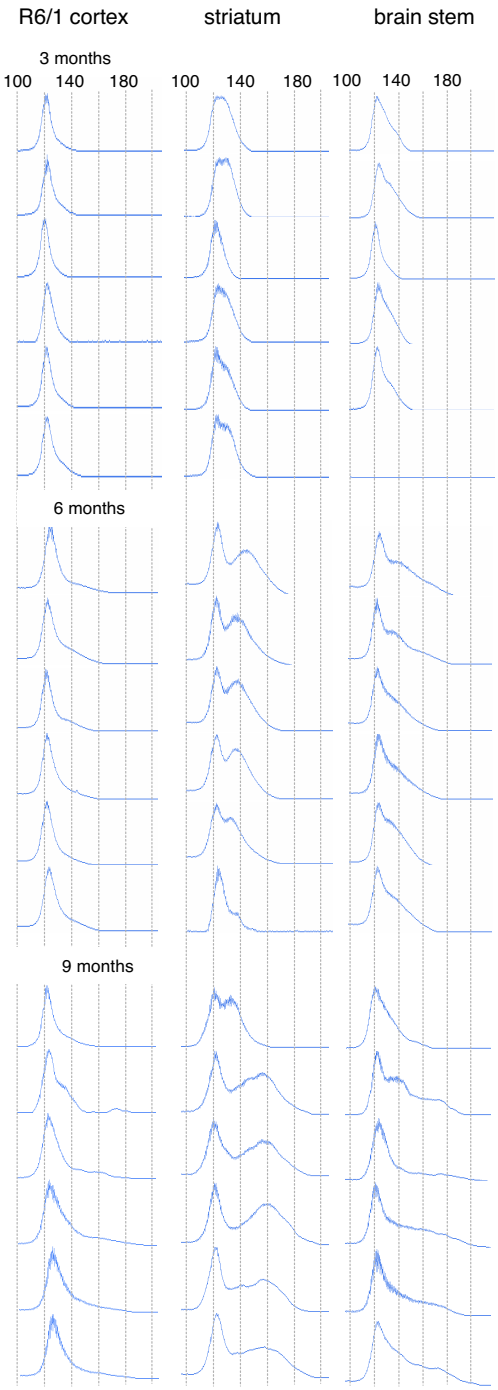


**Fig. 1.** Progression of CAG repeat instability is region-specific and comparable between mice. Each row is a compilation of ABI377 traces representing tissues taken from the same R6/1 mouse. Mosaicism is apparent by 3 months and progressively develops toward expansion with age. The three regions exhibit differing levels of instability: the striatum contains the largest proportion of expansions within its population of CAG repeats; the brainstem has the widest range of expansions; and instability in the cortex is more modest but still detectable. The overall shape of the repeat distribution is conserved between mice for the same brain region with the variance increasing with age. In both striatum and brainstem, the multimodal nature of the radical component of the traces is apparent at 9 months (also see Figs. 2 and 3). *x* axis, CAG repeat length as indicated; *y* axis, allele abundance.

transcribed from the R6/1 locus at 9 months of age. We found that the ranges but not the profiles of the CAG distributions are well matched between DNA and RNA (Fig. 3). The expression levels of the CAG repeat-bearing transcripts are mode-specific. In the striatum the impact of instability on the gene product is particularly pronounced, because this mode specificity acts to reverse the polarity of the profile between the DNA and RNA traces with repeats of the radical component being more highly expressed. The predominant mode in the RNA has a peak of 160 CAG repeats, which represents an increase of ≈36% over the peak of the conservative component. Expression disequilibrium between alleles and the high rate of instability in the striatum would cumulatively drive the pathogenic length of the CAG repeat in the HD gene product upwards and be expected to enhance its toxicity.

**Differential Distribution of the Radical and Conservative Components Between Brain Cell Types.** We observed that CAG repeat size distributions are composed of distinct populations of alleles, each with a differential level of expression. It has been documented that the level of HD gene expression is higher in neurons than in glia (16). It would, therefore, be consistent for striatal neurons to contain the radical component of instability. We used laser microdissection to isolate neuronal and nonneuronal populations and determined the associated CAG repeat distributions in the striata of R6/1 mice (Fig. 4*A*). Remarkably, at 6 months of age, the neuronal traces are composed mostly of the radical component. By 9 months, the entire neuronal distribution has migrated, while preserving its profile, as the alleles expand in a synchronous manner. The nonneuronal traces are composed mainly of the conservative component with a minor radical component that migrates with age at a rate similar to that of the neuronal distribution.

**CAG Repeats Are Unstable in Terminally Differentiated Neurons.** The progressive synchronized increase in the neuronal CAG repeat size suggests that the mutation is ongoing in postmitotic neurons in the absence of DNA replication and cell division. However, evidence of neurogenesis has been reported in rodent brain (17). To establish how the samples from which our data were derived relate to the total population of striatal neurons we evaluated our sampling methods. If our traces reflect the total population then they will be reproducible in independent PCRs. If they are not representative, they will differ according to a Poisson distribution. To test this, the PCR amplification of each dissected neuronal specimen was replicated (SI Fig. 7). The CAG profiles corresponded to the radical component and were reproducible within samples and between mice. This reproducibility testifies that the traces are representative of the CAG repeats of the total neuronal population in the striatum. For the expansion of the neuronal CAG alleles between the ages of 6 and 9 months to be explained by neurogenesis, most neurons would have to have divided during this period. However, it has been estimated that in the rat and mouse adult brain one neuron is produced each day for every 2,000 existing neurons (17), i.e., 0.05% per day. Over 90 days this would amount to only ≈4.5% of the total population of neurons. Reports of decreased neurogenesis in R6/1 mice (18) supports our conclusion that we have characterized nondividing cells and that we present direct evidence for CAG repeat instability in postmitotic neurons.

**Cellular Distribution of the CAG Mosaicism in HD Patient Brains.** A similar dissociation of the radical and conservative components of the CAG repeat distribution between the cell types can be observed in HD patient striata (Fig. 4*B*). The median CAG repeat lengths showed significant differences between neuronal and nonneuronal populations: HC104, neuronal 76.5, nonneuronal 54; HC73, neuronal 69, nonneuronal 51 (Kolmogorov–Smirnov $Z$ test, two-tailed comparison of neuronal and nonneuronal distributions: HC104, $Z = 3.253$, $P < 0.001$; HC73, $Z =$

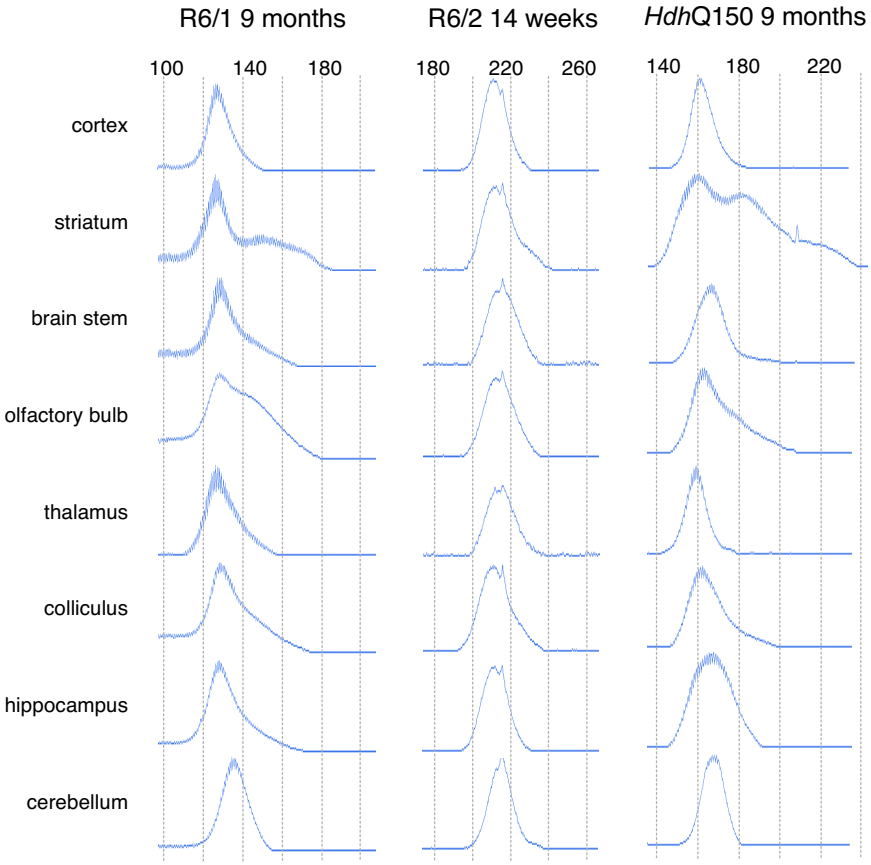


**Fig. 2.** Comparison of region-specific signatures of DNA instability among three HD mouse models. In both the R6/1 and *Hdh*Q150 models at 9 months of age, the most pronounced mosaicism can be seen in the striatum, olfactory bulb, colliculus, and cerebellum. Although the CAG sizes differ, the overall shape of the traces is preserved. The potential for the development of similar region-specific distributions is apparent in R6/2 mice at 14 weeks of age (end-stage disease) where mosaicism in the striatum and cerebellum can already be observed.

2.619, $P < 0.001$). Although the progression of repeat instability with age is difficult to establish in patients, it is reasonable to propose that, as in mouse, instability occurs in postmitotic neurons.

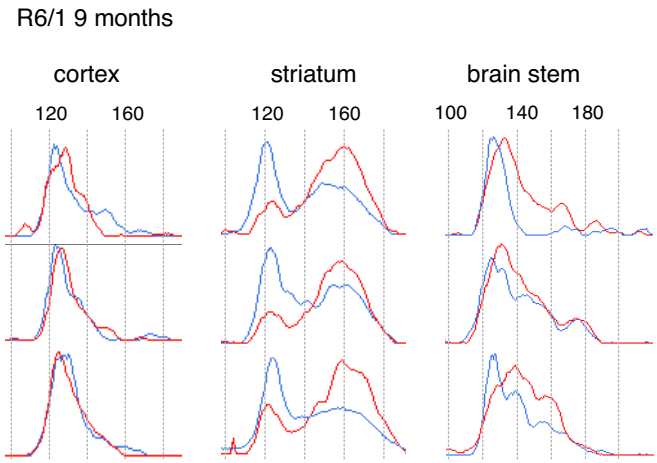


**Fig. 3.** Region-specific signatures of DNA instability and allele expression. Shown is a comparison of CAG repeat traces from DNA and RNA that have been extracted from the striata of the same R6/1 mouse at 9 months of age ($n = 3$). As for DNA, the region-specific RNA traces are consistent between mice. The DNA and RNA CAG repeat ranges are comparable and are composed of a number of peaks indicative of the multimodal nature of the radical component. The position but not the relative height of the peaks is conserved between the DNA and RNA traces. Therefore, the relative RNA allele abundance is the product of mode-specific expression levels. Note that there is no consistent relationship between the repeat length and respective expression level. Blue traces, DNA; red traces, RNA.

**Cell Specificity of MSH3 Distributions Correlates with Instability Rates and Is Conserved Between Humans and Mice.** The factors that cause the cell-specific differences in CAG repeat instability are unknown. Development of instability has been tightly linked to the mismatch repair pathway (7, 19–21). MSH2 expression is necessary for the development of instability in HD mice (7, 19), and its complex with MSH3 and not with MSH6 is required for instability (20). Because nothing is known about the cellular distribution of MSH3 in the brain, we performed immunohistochemistry and confocal microscopy to examine this in both human and mouse. Our colocalization studies detected MSH3 in the neuronal cells but not in the majority of nonneuronal cells of both mouse and human striatum (Fig. 5 and SI Fig. 8). Because cells in which MSH3 is absent are unable to modulate CAG repeat size with age in adulthood (20), the neuronal expression of this protein accounts for cell specificity of expansion in the striatum. Conservation of the colocalization of the radical component of CAG instability and MSH3 in neurons of mice and humans suggests that the observed mosaicisms are generated by the same mechanism. By extension, the neuronal mosaicism observed in humans is likely to have developed postmitotically.

## Discussion

We have shown that specific brain regions exhibit characteristic signatures of CAG repeat length distribution across different mouse models of HD. We established that these signatures evolve as a function of the differential rates of CAG instability occurring in the range of cell populations of which each brain region is composed. We found CAG repeats in terminally differentiated neurons of the adult mouse striatum to expand in synchrony between cells. Given the known dependence of CAG repeat instability on the mismatch repair system, our demonstration that repeats are somatically unstable in the cells where

GENETICS

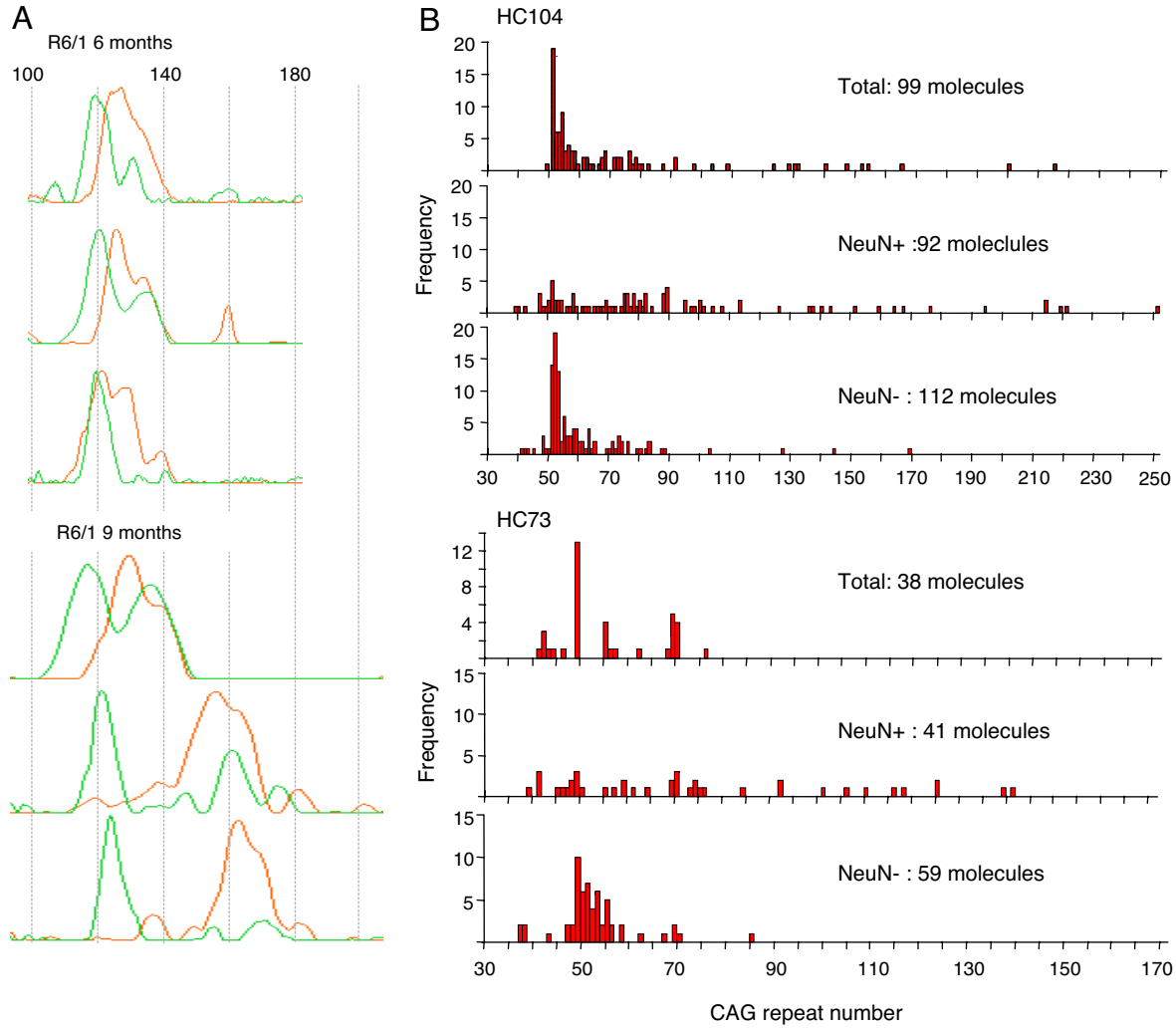


**Fig. 4.** Differential instability rates in neuronal and nonneuronal cells from human and mouse HD striata. (*A*) Neuronal and nonneuronal cells in R6/1 striatum were distinguished by NeuN antibody staining and isolated by laser microdissection. The superimposed traces from neuronal and nonneuronal populations display an obvious difference by 6 months. Adult neuronal cells almost exclusively carry somatically expanded alleles. There is greater heterogeneity in the nonneuronal profile, which might reflect the greater heterogeneity of cell types. Green traces, nonneuronal cells; orange traces, neuronal cells. (*B*) Cell populations were isolated from human patient striata as for mouse, and the CAG repeat distributions were complied by small-pool PCR. The extent of CAG mosaicism is greatest in the neuronal cell populations.

MSH3 is present at least partially explains how these cell-specific differences arise.

The length of the CAG repeat is proportional to the severity of the phenotype in model systems of HD (14, 22) and is negatively correlated to age of onset in HD patients (23). Because expression of the mutant allele is necessary for disease (24) the demonstration that somatically expanded alleles are expressed must link CAG instability to pathology. We show that striatum is distinguished from cortex and brainstem by a higher repeat length in mRNA as a result of high levels of CAG instability and neuronal expression levels. Although the functional consequence of this instability has not been quantified, the median difference in CAG size between neuronal and nonneuronal populations in human HD striatum would produce a difference of several decades in age of onset if analogous repeat lengths were inherited. We do not suggest that somatic CAG repeat instability is necessary for disease, because pathogenicity of the HD gene depends on many factors including CAG repeat length, gene expression level, huntingtin processing, and cellular context (a broad term encompassing protein folding and degradation networks among other cellular processes). Instead, we propose that instability acts as a significant disease modifier. In support of this, the rate of somatic instability has been shown to correlate with huntingtin accumulation in neuronal nuclei (7) although other factors clearly also contribute to this process (25).

We have found that striatal cell populations exhibit differential synchronized rates of CAG repeat instability and that therefore these must be driven by intrinsic cell-specific transacting factors. We have shown that MSH3 distribution contributes to this cell specificity. It has previously been demonstrated that MSH3 is absolutely necessary for instability *in vivo* (20) and that therefore the presence of MSH3 in neurons and its absence from most nonneuronal cells is highly significant. However, the wide variation in CAG instability between different brain regions predicts that the instability rate is governed by the mismatch repair system acting in conjunction with other factors. Oxidative damage is a possible candidate because this has been shown to modify instability rates (26). Recent experiments in *Drosophila* proposed that CAG instability is linked to pathogenesis (27). Our finding, that the CAG repeat signatures are comparable between R6/1 and *Hdh*Q150 mice at 9 months of age, when R6/1 mice are at end-stage disease and the *Hdh*Q150 knockins remain unaffected (15), contradicts this prediction and indicates

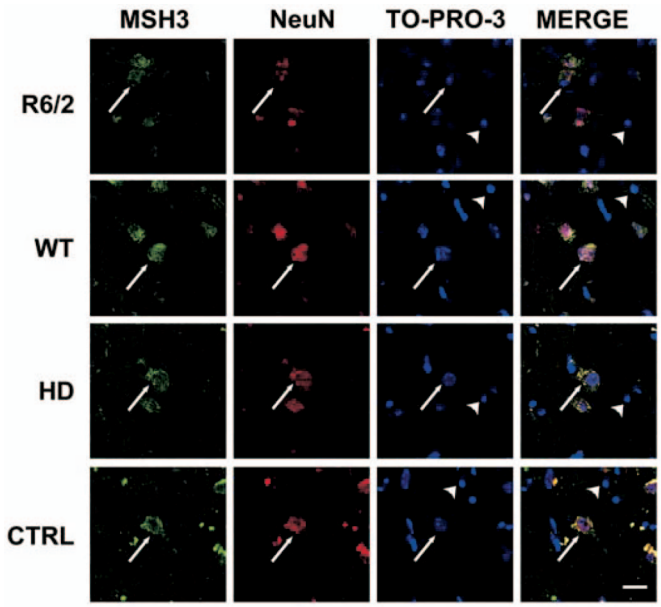


**Fig. 5.** MSH3 is present in neuronal cells in the human and mouse striatum. Sections of R6/1 and WT mice aged 9 months and from HD and control human striatum were immunoprobed with antibodies to NeuN to identify neurons and to MSH3. All nuclei were visualized by using TO-PRO-3. MSH3 is predominantly found in neurons in both mouse and human striata. Arrows, neuronal cells; arrowheads, nonneuronal cells. (Scale bar: 20 $\mu$m.) (See SI Fig. 8 for larger version).

that instability occurs as a consequence of age-related events that are little influenced by pathogenic cellular phenotypes.

We have shown that DNA hypermutation can take place in postmitotic neurons *in vivo*. Segregation and accumulation of functional alleles to produce a genetically distinct population of cells has been known to occur through selection and clonal proliferation (e.g., cancer or adaptive immune response). Here we show that it can occur through synchronous mutation in a significant population of postmitotic neurons. As a result of these phenomena, we show that cells in the brain diverge into genetically distinct groups as determined by the length of the CAG repeat. In the traditional view, random variation is produced throughout the genome between different cells. Even in adaptive immune response, random variations are produced within a region and are filtered through selection and clonal proliferation. For expansion of the neuronal CAG alleles to be synchronized, this mutation must be a deterministic response to a set of conditions that occur in separate cells. However, this is not adaptive (28), because the mutation is unlikely to optimize gene function in response to a selective environment.

We suggest that DNA may also be somatically unstable at other hypermutable tandem DNA repeat sequences and possibly other mutational hotspots in terminally differentiated cells. Such loci would have to have high mutation rates similar to those of the CAG repeats described here. It is known that variation in certain tandem DNA repeats can influence behavioral (2) and morphological (1) phenotypes. Therefore, it might be possible to identify hypermutable repeat loci that would contribute to diversification of characteristics in nondividing cells, thereby generating phenotypic variability outside of the disease setting.

## Methods

**Source of Mouse and Human Tissue.** Hemizygous R6/1 and R6/2 mice (13) were bred and reared in our colony by backcrossing R6 males to (CBA×C57BL/6) $F_1$ females (B6CBAF1/OlaHsd; Harlan Olac) as previously described (29). *Hdh*Q150 heterozygotes (original nomenclature: CHL2) on a mixed C57BL/6/129Ola (HM1 ES cells) background were generated at the University of Alabama (14). Frozen human brain tissue was from the New Zealand Neurological Foundation Brain Bank (University of Auckland). The study was approved by the St. Thomas's Hospital Research Ethics Committee. HD brains: HC104, male, age 40, grade 3 pathology, 18/51 CAG; HC73, male, age 47, grade 2 pathology, 19/49 CAG.

**DNA Extraction, RNA Extraction, and CAG PCR Amplification.** DNA was prepared by phenol/chloroform extraction except for the laser-dissected material, which was extracted by boiling in 0.25 M KCl/0.05 M DTT for 10 min. RNA was prepared by using the RNeasy Mini Kit (Qiagen) and reverse transcribed. The detailed conditions used to amplify the CAG repeat from R6/1, R6/2, and *Hdh*Q150 mouse DNA and human DNA are described in *SI Methods*.

**Repeat Sizing by ABI 377.** PCR amplification conditions were optimized to detect both small-pool and conventional PCR by using the ABI377 sequencer (SI Fig. 9). The protocol is detailed in *SI Methods*.

**Laser Microdissection.** Isolation of cellular populations was performed by using pressure-assisted laser microdissection. Frozen brain sections (15 $\mu$m) were mounted onto PEN1 membrane-covered slides (pressure-assisted laser microdissection). Sections were fixed in 90% ethanol and immunostained with NeuN antibody (1:200; Chemicon) as previously described (15) except that both primary and secondary antibody incubations were at room temperature for 20 min. Sections were washed and counterstained with methyl green. Conventional light microscopy (×40 objective) was used to collect the cell population of interest after all other cells had been ablated from the section.

**Immunohistochemistry and Confocal Microscopy.** Immunohistochemistry for confocal microscopy was as previously described (30). Primary antibody dilutions were MSH3 (pAb, 1:50; Santa Cruz Biotechnology) and NeuN (mAb, 1:200; Chemicon), and fluorescent secondary antibodies (Molecular Probes) were Alexa Fluor 488 donkey anti-goat (1:1,000) and Texas red goat anti-mouse (1:400). Nuclei were visualized by using TO-PRO-3 (Molecular Probes).

**Small-Pool PCR.** Small-pool PCR allows an exact description of the distribution of repeat lengths because their frequency can be measured directly by counting each single band as a single allele of a particular size (31). Each reaction contains a very small amount of template DNA so that individual alleles can be distinguished. We demonstrated that amplification of the CAG repeats from the striatum of an R6/1 mouse aged 9 months using both bulk PCR and small-pool PCR generated comparable repeat distributions (SI Fig. 10).

**ACKNOWLEDGMENTS.** This work was supported by the Medical Research Council and the Wellcome Trust (Grants 60360 and 66270).

1. Fondon JW, III, Garner HR (2004) Molecular origins of rapid and continuous morphological evolution. *Proc Natl Acad Sci USA* 101:18058–18063.
2. Hammock EA, Young LJ (2005) Microsatellite instability generates diversity in brain and sociobehavioral traits. *Science* 308:1630–1634.
3. Wells RD, Ashizawa T (2006) *Genetic Instabilities and Neurological Diseases* (Elsevier, San Diego).
4. Bates GP, Mangiarini L, Mahal A, Davies SW (1997) Transgenic models of Huntington's disease. *Hum Mol Genet* 6:1633–1637.
5. Mangiarini L, *et al.* (1997) Instability of highly expanded CAG repeats in mice transgenic for the Huntington's disease mutation. *Nat Genet* 15:197–200.
6. Kennedy L, Shelbourne PF (2000) Dramatic mutation instability in HD mouse striatum: Does polyglutamine load contribute to cell-specific vulnerability in Huntington's disease? *Hum Mol Genet* 9:2539–2544.
7. Wheeler VC, *et al.* (2003) Mismatch repair gene Msh2 modifies the timing of early disease in Hdh(Q111) striatum. *Hum Mol Genet* 12:273–281.
8. Telenius H, *et al.* (1994) Somatic and gonadal mosaicism of the Huntington disease gene CAG repeat in brain and sperm. *Nat Genet* 6:409–414, and erratum (1994) 7:113.
9. Kennedy L, *et al.* (2003) Dramatic tissue-specific mutation length increases are an early molecular event in Huntington disease pathogenesis. *Hum Mol Genet* 12:3359–3367.
10. Watanabe H, *et al.* (2000) Differential somatic CAG repeat instability in variable brain cell lineage in dentatorubral pallidoluysian atrophy (DRPLA): A laser-captured microdissection (LCM)-based analysis. *Hum Genet* 107:452–457.
11. Hashida H, *et al.* (2001) Single cell analysis of CAG repeat in brains of dentatorubral-pallidoluysian atrophy (DRPLA). *J Neurol Sci* 190:87–93.
12. Shelbourne PF, *et al.* (2007) Triplet repeat mutation length gains correlate with cell-type specific vulnerability in Huntington disease brain. *Hum Mol Genet* 16:1133–1142.
13. Mangiarini L, *et al.* (1996) Exon 1 of the HD gene with an expanded CAG repeat is sufficient to cause a progressive neurological phenotype in transgenic mice. *Cell* 87:493–506.

14. Lin CH, *et al.* (2001) Neurological abnormalities in a knock-in mouse model of Huntington's disease. *Hum Mol Genet* 10:137–144.
15. Woodman B, *et al.* (2007) The Hdh(Q150/Q150) knock-in mouse model of HD and the R6/2 exon 1 model develop comparable and widespread molecular phenotypes. *Brain Res Bull* 72:83–97.
16. Landwehrmeyer GB, *et al.* (1995) Huntington's disease gene: Regional and cellular expression in brain of normal and affected individuals. *Ann Neurol* 37:218–230.
17. Gage FH (2000) Mammalian neural stem cells. *Science* 287:1433–1438.
18. Lazic SE, *et al.* (2004) Decreased hippocampal cell proliferation in R6/1 Huntington's mice. *NeuroReport* 15:811–813.
19. Manley K, Shirley TL, Flaherty L, Messer A (1999) Msh2 deficiency prevents in vivo somatic instability of the CAG repeat in Huntington disease transgenic mice. *Nat Genet* 23:471–473.
20. van den Broek WJ, *et al.* (2002) Somatic expansion behaviour of the (CTG)n repeat in myotonic dystrophy knock-in mice is differentially affected by Msh3 and Msh6 mismatch-repair proteins. *Hum Mol Genet* 11:191–198.
21. Owen BA, *et al.* (2005) (CAG)(n)-hairpin DNA binds to Msh2-Msh3 and changes properties of mismatch recognition. *Nat Struct Mol Biol* 12:663–670.
22. Morley JF, Brignull HR, Weyers JJ, Morimoto RI (2002) The threshold for polyglutamine-expansion protein aggregation and cellular toxicity is dynamic and influenced by aging in *Caenorhabditis elegans*. *Proc Natl Acad Sci USA* 99:10417–10422.
23. Myers RH, Marans KS, MacDonald ME (1998) in *Genetic Instabilities and Hereditary Neurological Diseases*, eds Wells RD, Warren ST (Academic, San Diego), pp 301–323.
24. Yamamoto A, Lucas JJ, Hen R (2000) Reversal of neuropathology and motor dysfunction in a conditional model of Huntington's disease. *Cell* 101:57–66.
25. Lloret A, *et al.* (2006) Genetic background modifies nuclear mutant huntingtin accumulation and HD CAG repeat instability in Huntington's disease knock-in mice. *Hum Mol Genet* 15:2015–2024.
26. Kovtun IV, *et al.* (2007) OGG1 initiates age-dependent CAG trinucleotide expansion in somatic cells. *Nature* 447:447–452.
27. Jung J, Bonini N (2007) CREB-binding protein modulates repeat instability in a Drosophila model for polyQ disease. *Science* 315:1857–1859.
28. Cairns J, Overbaugh J, Miller S (1988) The origin of mutants. *Nature* 335:142–145.
29. Hockly E, Woodman B, Mahal A, Lewis CM, Bates G (2003) Standardization and statistical approaches to therapeutic trials in the R6/2 mouse. *Brain Res Bull* 61:469–479.
30. Smith DL, *et al.* (2001) Inhibition of polyglutamine aggregation in R6/2 HD brain slices—Complex dose-response profiles. *Neurobiol Dis* 8:1017–1026.
31. Jeffreys AJ, *et al.* (1994) Complex gene conversion events in germline mutation at human minisatellites. *Nat Genet* 6:136–145.